



Article

Physicochemical and Mineralogical Characterizations of Two Natural Laterites from Burkina Faso: Assessing Their Potential Usage as Adsorbent Materials

Corneille Bakouan 1,2,3, Louise Chenoy 3, Boubié Guel 2,*, and Anne-Lise Hantson 3

- Laboratoire de Recherche et de Développement (LRD), Université Lédéa Bernard Ouédraogo, Ouahigouya 01 BP 346, Burkina Faso; bakouancorneille@gmail.com
- Laboratoire de Chimie Moléculaire et des Matériaux (LCMM), Université Joseph Ki-Zerbo, U.F.R-SEA/, Ouagadougou 03 BP 7021, Burkina Faso
- Service de Génie des Procédés Chimiques et Biochimiques, Faculté Polytechnique, Université de Mons, Place du Parc 20, 7000 Mons, Belgium; louise.chenoy@umons.ac.be (L.C.); anne-lise.hantson@umons.ac.be (A.-L.H.)
- * Correspondence: boubieguel@yahoo.fr or boubie.guel@ujkz.bf; Tel.: +226-76645044

Abstract: In the framework of lateritic material valorization, we demonstrated how the geological environment determines the mineralogical characterizations of two laterite samples, KN and LA. KN and LA originate from the Birimian and Precambrian environments, respectively. We showed that the geological criterion alone does not determine the applicability of these laterites as potential adsorbents but must be associated with their physicochemical properties. The characterizations were carried out using Fourier transform infrared spectroscopy (FTIR), X-ray diffraction (XRD), Thermal analysis, and Atomic Emission Spectrometry Coupled with an Inductive Plasma Source. The major mineral phases obtained by X-ray diffraction analysis coupled with infrared analysis showed that the KN and LA laterite samples were composed of quartz (33.58% to 45.77%), kaolinite (35.64% to 17.05%), hematite (13.36% to 11.43%), and goethite (7.44% to 6.31%). The anionic exchange capacity of the KN and LA laterites ranged from 86.50 ± 3.40 to 73.91 ± 9.94 cmol(-)·kg⁻¹ and from 73.59 ± 3.02 to 64.56 ± 4.08 cmol(-)·kg⁻¹, respectively, and the cation exchange capacity values are in the order of 52.3 ± 2.3 and 58.7 ± 3.4 cmol(+)/Kg for the KN and LA samples, respectively. The specific surface values determined by the BET method were 58.65 m²/g and 41.15 m²/g for the KN and LA samples, respectively. The effects of adsorbent doses on As(III,V), Pb(II), and Cu(II) adsorption were studied. At 5 mg/L As and 15 g/L adsorbent (pH 6.5–7), arsenate removal was 99.72 \pm 0.35% and 99.58 \pm 0.45% for KN and LA, respectively, whereas arsenite removal reached 83.52 \pm 2.21% and 98.59 \pm 0.64% for LA and KN, respectively. The Pb(II) and Cu(II) removal rates were $74.20 \pm 0.95\%$ for 2.4 g/LKN and $54.18 \pm 0.01\%$ for 8 g/L KN, respectively. Based on their physicochemical and mineralogical characteristics, the KN and LA laterite samples were shown to possess a high potential as adsorbent material candidates for removing heavy metals and/or anionic species from groundwater.

Keywords: natural laterites; sorption properties; mineralogy; anionic exchange capacity



Academic Editors: Elisa Laita, Javier García-Rivas and Isabel Abad

Received: 25 February 2025 Revised: 28 March 2025 Accepted: 2 April 2025 Published: 4 April 2025

Citation: Bakouan, C.; Chenoy, L.; Guel, B.; Hantson, A.-L. Physicochemical and Mineralogical Characterizations of Two Natural Laterites from Burkina Faso: Assessing Their Potential Usage as Adsorbent Materials. *Minerals* 2025, 15, 379. https://doi.org/10.3390/ min15040379

Copyright: © 2025 by the authors. Licensee MDPI, Basel, Switzerland. This article is an open access article distributed under the terms and conditions of the Creative Commons Attribution (CC BY) license (https://creativecommons.org/licenses/by/4.0/).

1. Introduction

Laterites constitute a large family of soils typical of humid tropical regions. They originate from the alteration process of a bedrock, which is depleted in silica and enriched in iron oxide and alumina. They are products of intense meteoric weathering and consist of a mineral assemblage of goethite, hematite, aluminum hydroxide, kaolinite, and quartz [1–3].

Chemically, the structure of lateritic materials contains a high percentage of iron oxide (Fe_2O_3) , alumina (Al_2O_3) , and silica (SiO_2) mineral phases, which are present as a combination consisting of $Fe_2O_3 - Al_2O_3 - SiO_2 - H_2O$ matrices [3]. The $SiO_2/(Al_2O_3 + Fe_2O_3)$ ratio compared to that of the parent rock must be in such a way that the laterite formation does not contain more silica than the one which is retained in the remaining quartz and which is only necessary for the formation of kaolinite [4]. Moreover, laterites occur in nature with various yellow, brown, and red residual solids of nodular gravels and fine-grained and/or cemented solids. Laterites can vary from loose red sand to massive hard rock; sometimes, both forms coexist. The characteristic red color appears due to the presence of iron compounds in laterite. The physicochemical and mineralogical properties of laterite vary considerably depending on the extent of lateralization, the parent rock, and the geological environment [5,6].

The mineralogical composition, including minerals such as kaolinite and hematite, influences the chemical reactivity of laterites, determining their ability to interact with metal ions. Moreover, the geological environment of certain laterites can make them more effective at removing pollutants. Understanding these properties is essential for assessing their potential in the remediation of contaminated waters.

Laterites have been the subject of diverse applications reported in the literature [7-12]. They have been widely used in road construction in tropical and equatorial African countries, as well as in South America, whether they are lateritic gravels, lateritic clays, lateritic shells, or crusts [1,13,14]. They were also shown to be efficient adsorbents in treating water contaminated by inorganic pollutants. In several countries such as India, Vietnam, and Bangladesh, they have been used with great satisfaction in the adsorption of arsenic [8,9,15-17]. We recently reported their application for arsenic removal in Burkina Faso [2]. According to the literature, the efficiency of these materials as the best adsorbent candidates for the removal of inorganic and organic pollutants is only highlighted by their physicochemical and structural characteristics: the specific surface area, the anionic exchange capacity, the cation exchange capacity, and the composition, which is made up mostly of iron and aluminum oxides. These characteristics appeared to be the most critical and were highlighted in several studies on clay and/or lateritic minerals used to remove inorganic or organic pollutants [11,12,18-20]. Their applications depend closely on their structure, composition, and physicochemical characteristics. Being aware of these characteristics is decisive for better exploitation and probably opens up new application areas [21]. On the one hand, upon reviewing papers published in the last ten years, it was found that most of the studies did not cover the gap between the environmental perspective of the laterites, as adsorbent materials, and their physicochemical properties. On the other hand, the development of lateritic material-based environmental applications constitutes a relevant research area that contributes to their economical valorization. From this environmental perspective, any research that demonstrates the great potential of laterites to address practical environmental problems, such as the removal of arsenic and/or heavy metal ions from aqueous solutions, should highlight the fact that those applications depend closely on their structure, their mineralogical composition as determined by the geological environment, and their physicochemical properties. The present work focuses on this correlation, unlike most publications in which the emphasis is not placed on physicochemical properties, such as the cation exchange capacity (CEC) and the anionic exchange capacity (AEC).

In the literature, various techniques, such as X-ray powder diffraction, Fourier transform infrared (FT-IR) spectroscopy, scanning electron microscopy (SEM), chemical analysis, cation exchange capacity (CEC), and specific surface area (BET) have been carried out to investigate the laterite characterization processes because of the removal of inorganic pollutants [7–11,22–24]. Although numerous studies have been conducted on the characteri-

Minerals **2025**, 15, 379 3 of 24

zation of natural laterites for the sorption of heavy metal ions and/or metalloids [8,9,24–26], few of them have explored the relationship among their physicochemical and mineralogical properties, their adsorptive properties, and geological environment. Thus, given their interesting properties, laterite-based adsorbents can be particularly effective for the adsorption of heavy metal ions in aqueous solution.

Ghani et al. used a geopolymer based on lateritic clay as a potential adsorbent for the removal of heavy metals from aqueous solutions [23]. Zhu et al. effectively removed several heavy metals (As, Cr, Pb, Cu, Cd, and Hg) from wastewater using a new lateritic ceramic [27]. Mitra et al. also determined the characteristics of lateritic soil for its use in the removal of Pb(II) and Cr(VI) from synthetic wastewater [25]. He et al. found excellent behavior of a cost-effective limonitic laterite for the adsorption of Pb(II) and Cd(II) hydrates [24]. Mohapatra et al. studied the adsorption of lead (II) from contaminated waters using Indian nickel laterite ores [26]. Although numerous papers have been published in this field, we noted that the previous studies are not exhaustive. To the best of our knowledge, this study is the first to provide a complete description of laterite properties, in terms of specific surface area, pore volume, DSC/TGA, PZC, chemical composition, mineralogical characterization, cation exchange capacity (CEC), and anionic exchange capacity (AEC), in relation to the adsorption ability of the material. Indeed, these properties are helpful criteria that provide strong evidence of the adsorption capacity of the laterites regarding the removal of cationic and/or anionic pollutants from aqueous solutions.

The geological map of the country is divided into square degrees depending on the nature of the rocks and their structure, which facilitates the understanding of the distribution of resources, notably the lateritic sites. We initially selected four laterites (KN, LA, BN, and DA) based on the specific geological characteristics of each square degree. Experiments were conducted on these four laterites rich in iron and aluminum oxides, which are crucial for environmental applications, such as the removal of arsenic and/or heavy metal ions from aqueous solutions. The results obtained for the DA laterite were satisfactory since in the batch mode, we achieved an elimination rate of 97.30% for As(III) at a dose of 0.75 g of laterite [2]. The adsorption capacity was 0.30 mg/g [2]. These investigations paved the way for the first uses of local natural laterites from Burkina Faso for As(III) remediation from drinking water using fixed-bed columns [28]. We also achieved an elimination rate of 99.69% for As(V) at a dose of 0.75 g of laterite [2]. The adsorption capacity for DA laterite was 0,33 mg/g [2]. The results obtained with BN laterite were not satisfactory due to the low content of iron and aluminum oxides. The present paper provides the results obtained with the KN and LA laterites that were chosen on the basis of their geological environment, so as to be rich in iron and aluminum oxides.

This study aims to determine (i) the physicochemical and structural characteristics of the two KN and LA natural laterites, by using various techniques, such as XRD, FTIR, SEM + EDX, DSC, CEC, and AEC; and (ii) the correlation between their physicochemical and structural characteristics and their potential usage as adsorbent materials. This work makes it possible to determine how the physicochemical properties of these natural laterites predispose them to be potential adsorbent materials, thereby contributing to the sustainable management of the natural lateritic resources.

2. Materials and Methods

2.1. Origin of Samples

Laterite samples were collected from two distinct sites of Burkina Faso (Figure 1). The first one, named KN, was collected in the northern part of Kaya, at the following coordinates: $13^{\circ}07'13.47''$ N and $1^{\circ}06'52.28''$ W. The second one, named LA, was collected

Minerals **2025**, 15, 379 4 of 24

in Laye village, at the following coordinates: $12^{\circ}31'27.05''$ N and $1^{\circ}47'07.22''$ W. The laterite from KN is light red, and the one from LA is red-brown.

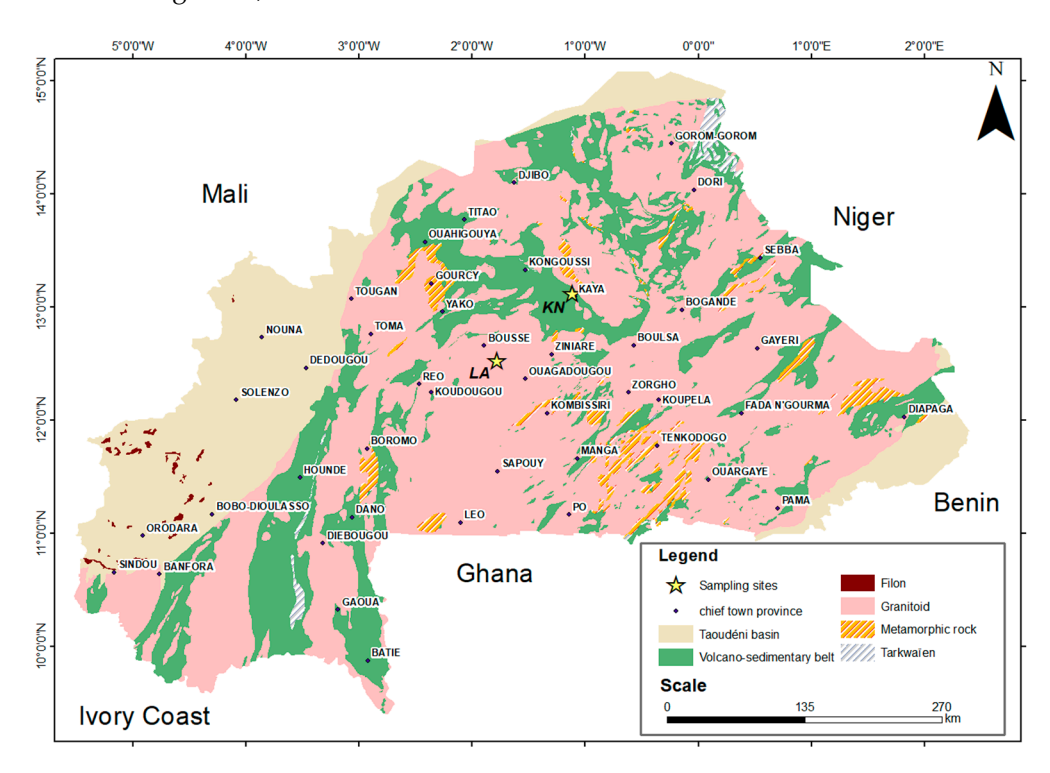


Figure 1. Location of collected laterite samples.

The term "Tarkwaien" refers to specific geological formations, typically associated with gold deposits, primarily located in West Africa. Tarkwaien deposits are usually metamorphic rock formations, often composed of quartzite and schist. These rocks are formed under high pressure and temperature conditions [29].

2.2. The Specific Geological Contexts of the Sites

The territory of Burkina Faso is divided into square degrees, and each site belongs to a square degree. The geological details of these square degrees are shown on the various positioning maps produced for the different sites.

2.2.1. Geological Context of the Northern Kaya Site

This site belongs to the Kaya square degree, located between latitudes 1° and 1° north and longitudes 1° and 2° west. The geological formations are primarily composed of volcanic and volcano-sedimentary rocks (Figure 2). These rocks form relief areas, while the flat vast regions, at altitudes ranging from 300 to 350 m, comprise granitic materials such as protoliths. From a geological point of view, the KN samples originate from the environment of Birimian rocks, stemming from andesine (with a calcic-alkaline affinity), basalt, and dacit alteration.

Minerals **2025**, 15, 379 5 of 24

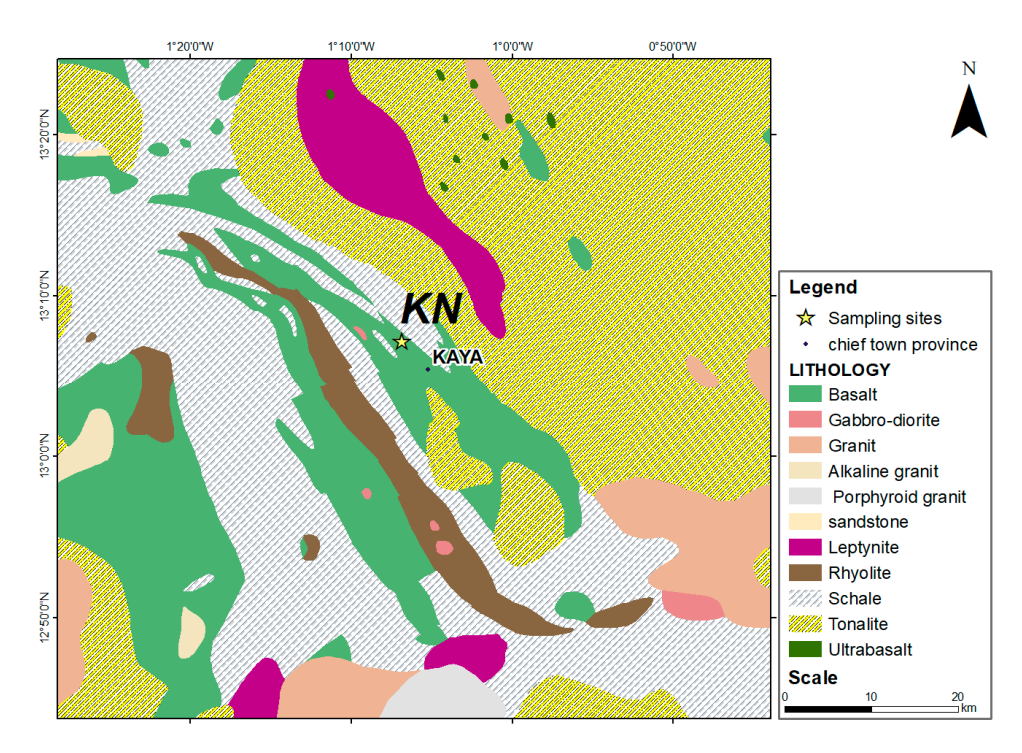


Figure 2. Geological map of northern Kaya laterite site.

2.2.2. Geological Context of the Laye Site

The Laye (LA) site belongs to the square degree of Ouagadougou and is located 35 km from Ouagadougou. The square degree of Ouagadougou is located between parallels 12 and 13° north latitude and meridians 1 and 2° west longitude. Unlike Kaya, this square degree is mainly composed of granite formations, corroborating its generally flat relief. The Laye site is located on highly indurated lateritic formations derived from a granitic protolith (alkaline granite). From a geological point of view, this area is located in an environment of Precambrian rocks (Figure 3).

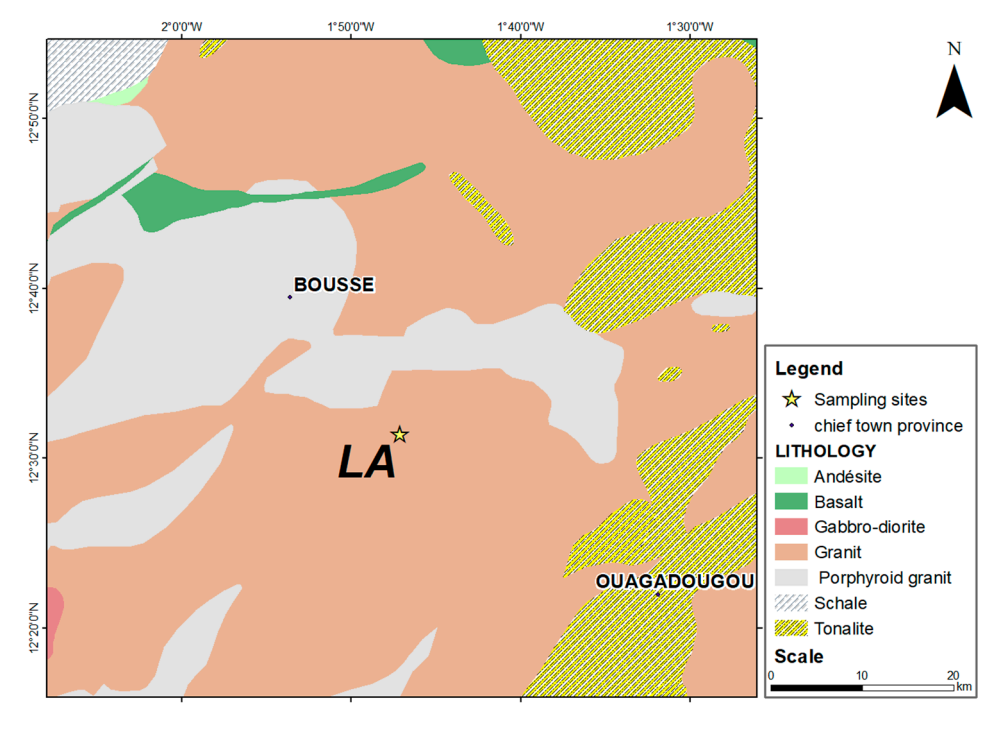


Figure 3. Geological map of Laye laterite site.

Minerals **2025**, 15, 379 6 of 24

2.3. Raw Material Characterization

2.3.1. Chemical Composition

Elementary chemical analysis was performed by ICP (ICP-AES-IRIS Intrepid II XSP model, detection limit = 9 μ g/L). A total of 0.25 g of laterite samples were digested in a microwave oven in 4 mL of HF (30% w/w), 3 mL of H₂SO₄ (96% w/w), and 3 mL of HNO₃ (65% w/w) [30].

2.3.2. Infrared Spectroscopy

Fourier transform infrared (FTIR) spectroscopy was performed using a Shimadzu FTIR-8400S spectrometer (FTIR-8400S spectrometer, Duisburg, Germany) to identify functional groups on the laterite samples. The spectra were acquired by accumulating 20 scans with a resolution of 4 cm⁻¹ over a wavelength range of 400 to 4000 cm⁻¹. Infrared analysis of the laterite samples was performed using the potassium bromide pelletizing technique. The pellets were made by mixing 5 mg of each sample with 500 mg of potassium bromide (KBr, Merck, Darmstadt, Germany). The mixture was finely ground and subjected to a pressure of ten (10) tons. The pellet thus formed was analyzed with a spectrophotometer.

2.3.3. X-Ray Powder Diffraction (XRD)

The structure, characteristics, and phase composition of the laterite samples were analyzed by X-ray diffraction analysis (XRD) on a SIEMENS D5000 equipment (KS Analytical Systems, Plano, TX, USA) running with the DIFFRAC AT software version 2.0 (Co-K α radiation (λ = 1.54060 Å); graphic monochromator; measurement in the 20 to 80 θ game; 40 kV voltage and 30 mA current).

2.3.4. Semi-Quantification

The semi-quantitative analysis of the different mineral phases was carried out by coupling the X-ray diffraction results with the chemical analysis results. This coupling allowed for the evaluation of the relative quantities of the minerals contained in the laterites using Equation (1) [2,31].

$$T(a) = \sum M(i) \times P_i(a) \tag{1}$$

T(a): content of the oxide "a" in the sample; Mi: content (%) of mineral "i" in the sample; $P_i(a)$: proportion of oxide "a" in mineral "i" (this proportion is deduced from the ideal formula assigned to mineral "i"). The quantitative approach was performed on the following basis:

- Alumina is distributed in kaolinite;
- Iron oxide is distributed between goethite and hematite;
- Silicon oxide is distributed between quartz and kaolinite.

The mass percentages of mineral elements were obtained from Equations (2)–(5).

$$\% Kaolinite = \% Al_2O_3 \times \frac{M_{Kaolinite}}{M_{Al_2O_3}}$$
 (2)

$$\%Quartz = \left(\%SiO_2 - \%Kaolinite \times \frac{M_{SiO_2} \times 2}{M_{Kaolinite}}\right) \times \frac{M_{Quartz}}{M_{SiO_2}}$$
(3)

$$\begin{array}{c} M_{(Goethite+Hematite)} \rightarrow \% Fe_2O_3 \\ M_{Goethite} \rightarrow \% Goethite \end{array} \tag{4}$$

$$\%Hematie = (\%Al_2O_3 - \%Goethite)$$
 (5)

Minerals **2025**, 15, 379 7 of 24

2.3.5. Differential Scanning Calorimetry (DSC) and Thermogravimetric Analysis (TGA)

Thermogravimetric and differential scanning calorimetry analysis was carried out on a TGA/DSC thermal analyzer (TGA/DSC1-STARe METTLER TOLEDO System, Zaventem, Belgium) under a nitrogen atmosphere at a heating rate of 10 °C/min. A mass of 5 g of raw laterite powder with a particle size of 106 μm was heated from 25 °C to 1500 °C. The TGA/DSC data were analyzed using the METTLER TOLEDO STARe software version 9.00.

2.3.6. Zeta Potential Measurements

Zeta potential measurements were performed to determine the electrostatic magnitude between the particles of the laterite samples. Zeta meter equipment (Zetasizer nano ZS, Malvern, Belgium) was used to measure the isoelectric point (IP) of the natural laterite samples. The pH solution was adjusted with $0.025 \, \mathrm{mol.L^{-1}}$ HCl and $0.025 \, \mathrm{mol.L^{-1}}$ NaOH solutions. The data were calculated using the software ZS (Malvern Panalytical, version 4.0).

2.3.7. Specific Surface Area and Porosity by Nitrogen Sorption Analysis

Nitrogen (N_2) sorption isotherms at 77 K were measured using the BelSorp-max instrument (Osaka, Japan) running with the Bel Japan Inc Surface Area and Porosity Analyzer. Before N_2 sorption measurements, the samples were vacuum-dried at room temperature for at least 24 h, followed by degassing under heating and vacuum, using a Sample Degas System. The value of each material's specific surface was determined with a device from Bel Sorp-max/Bel Japan.Inc (Osaka, Japan) brand controlled by Bel Japan software. Inc., version 1.3

2.4. Cation Exchange Capacity (CEC)

The cation exchange capacity was determined by shaking 0.5~g of the laterite sample with 30~mL of 0.05~mol/L hexaamminecobalt (III) chloride ($[Co(NH_3)_6]^{3+}$, $3Cl^-$) solution for 2 h. Before each determination of the CEC, a calibration curve was established using standard solutions ranging from 0.005~to~0.05~mol/L. This procedure creates a reference that links instrumental responses to known concentrations, allowing for reliable and reproducible measurements of CEC. The supernatant was collected and analyzed by SHIMADZU UV-visible spectrometry at 475 nm. The cation exchange capacity was calculated according to Equation (6).

$$C.E.C = \frac{(C_i - C_f) \times V}{m} \times 100$$
 (6)

 C_i and C_f are the initial and equilibrium concentrations of the hexaamminecobalt (III) chloride solution (mol/L), respectively; m is the mass of the laterite sample; and V is the volume of the solution.

2.5. Anionic Exchange Capacity (AEC)

The anionic exchange capacity (AEC) was determined by adapting the method proposed by Zelazny et al. to our study context [32]. It was determined at different pH values (pH framing the isoelectric point of the material) using chloride ions as an anionic index. The AEC measurement methods are based on the same principle as the cation exchange capacity (CEC) and are subject to the same constraints. All tests were carried out in triplicate.

Thus, 2 g of laterite was placed in a series of centrifugation tubes with a capacity of 50 mL. Then, 20 mL of CaCl₂ (0.1 mol/L) was added and left under gentle stirring for 1 h to saturate the laterite with chloride. After 1 h of stirring, the mixtures were centrifuged at 3000 rpm for 5 min, and the residues were recovered. The residues were rewashed five times with 20 mL of CaCl₂ (0.002 mol/L), left in contact for 1 h, and centrifuged for 5 min at

Minerals **2025**, 15, 379 8 of 24

3000 rpm. Then, 5 mL of CaCl₂ (0.002 mol/L), 1.5 mL of HCl (0.1 mol/L), and 3.5 to 5 mL of milli-Q water, respectively, were added so that the total volume was equal to 10 mL.

The suspensions were placed in a bath at 25° C for six days, shaking them manually, thrice daily. On the seventh day, the pH of each suspension was measured, and the mixture was centrifuged at 3000 rpm for 10 min. The chloride ions (C_1) were then evaluated. The mass of the residues and of the tube were weighed and recorded in order to determine the volume (V_1) of the solution that remained trapped.

The residues were resuspended in 30 mL of an ammonium nitrate solution (1 mol.L $^{-1}$), left in contact for 1 h, and then centrifuged at 3000 rpm for 10 min. The clear solution was recovered in a 100 mL volumetric flask (V_2). This operation was repeated twice, and the flasks' contents were adjusted with an ammonium nitrate solution (1 mol.L $^{-1}$). The chloride ions (C_2) were assayed in this final solution, and the anionic exchange capacity was determined by Equation (7).

$$AEC\left(cmol.kg^{-1}\right) = \left(C_2V_2 - C_1V_1\right) \times \frac{0.1 \times z}{M \times W} \tag{7}$$

were

 C_1 is the concentration (mg.L⁻¹) of Cl⁻ in the final washing solution of 0.1 M CaCl₂. C_2 is the concentration (mg.L⁻¹) of Cl⁻ in the displacing solution of 1 M NH₄NO₃.

 V_1 is the volume (mL) of the solution contained in laterites after the final washing of 0.1 M CaCl₂.

 V_2 is the total volume (mL) of the displacing solution 1 M NH₄NO₃.

M and z are the atomic weight and charge of Cl⁻, respectively.

W is the laterite sample's weight (g).

2.6. Experimental Studies on Arsenic and Heavy Metal Ion Removal

All arsenic and heavy metal ion (Cu and Pb) solutions were prepared with ultrapure water (milliQ-water, resistivity 18.2 M Ω .cm). The glass materials were preliminary immerged in diluted nitric acid (5% w/w) for at least 12 h and then rinsed with ultra-pure water. Arsenic (V) and arsenic (III) stock solutions of 1000 mg/L were prepared from Na₂HAsO₄ 7H₂O (98%, Alfa Aesar, Geel, Belgium) and NaAsO₂ (0.05 mol/L Alfa Aesar, Belgium), respectively. Pb(II) and Cu(II) stock solutions of 1000 mg/L were prepared from Pb(NO₃)₂ (\geq 99%, Merck, Darmstadt, Germany) and Cu(NO₃)₂ 3H₂O) (\geq 99%, Merck), respectively. All solutions were stored at 4°C. The working solutions for the experiments were freshly prepared by diluting the stock solutions.

All experiences were carried out in triplicate. The influence of the laterite sample dose on the arsenic adsorption was carried out under equilibrium conditions. In 250 mL polyethylene bottles, 50 mL As(III), As(V), Pb(II), and Cu(II) solutions of known concentrations were used with laterite samples at various quantities. Working solutions of 5 mg/L arsenic (III, V) were mixed with laterite samples varying from 2.5 g/L to 45 g/L. The solutions were agitated for 24 h at temperature of 18 ± 2 °C (overhead shaker Heidolph REAX-15 rpm, Schwabach, Germany). The solutions of Pb(II) (10 mg/L) or Cu(II) (10 mg/L) were mixed with variable mass samples of KN laterite. The masses ranged from 0.4 g/L to 3.2 g/L for Pb(II) and from 0.8 g/L to 16 g/L for Cu(II). The mixtures were stirred for 1 h and 30 min using a Heidolph REAX 20 mechanical stirrer at room temperature (18 ± 2 °C). Then, 14 mL of each filtrate was placed in 15 mL bottles, then acidified with 1 mL of nitric acid and stored at 4 °C before being analyzed by ICP-AES. Before each analysis, a ten-point calibration curve was established by successive dilution (5 ppm, 2.5 ppm, 1 ppm, 0.5 ppm, 0.25 ppm, 0.1 ppm, 0.05 ppm, 0.01 ppm, and 0.005 ppm, blank) using a commercial standard solution of 1000 ± 0.05 mg/L in 5% nitric acid.

Minerals **2025**, 15, 379 9 of 24

The equilibrium solutions were filtered through a 0.45 μ m nylon membrane (diameter 25 mm, VWR) after centrifugation (BECKMAN J2-MI model, Cincinnati, OH, USA) for 15 min at 3000 rpm and analyzed by ICP-AES (detection limit = 9 μ g/L). The percentage of removed As(III, V), Pb(II), and Cu(II) was determined according to Equation (8).

%Ads
$$(As(III, V); Pb(II); Cu(II)) = \frac{C_0 - C_e}{C_0} \times 100$$
 (8)

 C_0 and C_e are the initial and final concentrations (mg/L), respectively, of arsenic and heavy metal ions in the solutions.

3. Results and Discussion

3.1. Chemical Composition

The chemical composition in Table 1 indicates the major oxides (SiO_2 , Al_2O_3 , and Fe_2O_3) and the minor oxides (Na_2O , K_2O , TiO_2 , MgO, MnO_2 , and CaO) in the KN and LA samples. Other properties, such as the apparent density, total organic carbon (TOC), and organic matter (OM), are also shown in Table 1.

Table 1. Characteristics and composition (wt, %) of KN and LA laterite samples.

KN	LA
0.16	0.09
0.73	1.32
2.9	2.6
c composition (wt.%)	
20.8	17.65
14.09	6.74
50.16	53.70
1.70	1.82
1.43	1.40
2.10	2.10
0.65	0.95
0.35	0.68
0.70	0.75
8.01 ± 0.02	12.55 ± 0.23
99.99	98.34
	0.16 0.73 2.9 c composition (wt.%) 20.8 14.09 50.16 1.70 1.43 2.10 0.65 0.35 0.70 8.01 ± 0.02

L.O.I: loss on ignition.

According to the literature [13,33], iron is found as oxyhydroxides. Oxides of potassium, sodium, and titanium are in small amounts in both samples. These results suggest that quartz, aluminosilicates, and iron minerals are predominant in the samples studied. The low levels of potassium, sodium, and titanium oxides indicate that compounds containing titanium, potassium, and sodium are non-existent or present in tiny proportions. The elements in KN and LA are grouped according to their family in Table 2.

Table 2. Chemical composition of samples by type of elements in % by weight.

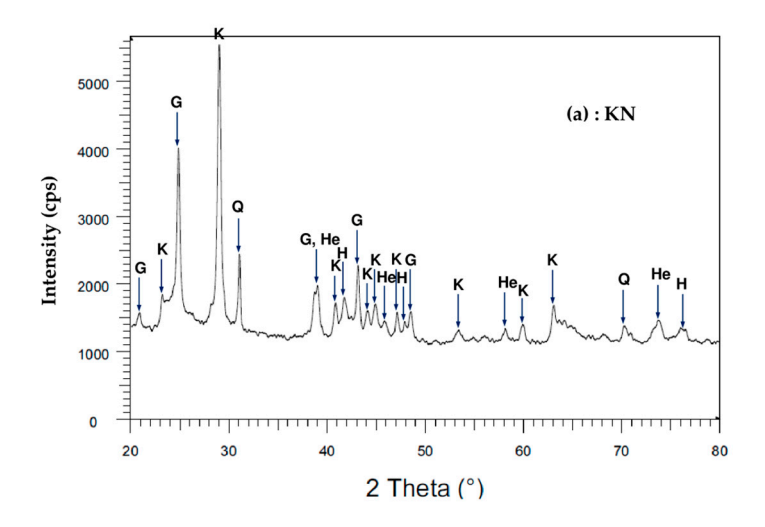
Family	Alkalis	Alkaline Earth	Metals	Silica
KN	3.1	0.1	37.3	50.2
LA	3.2	0.2	26.6	53.7

This study is the first to carry out this classification by type of elements, providing useful criteria of the elements present in lateritic materials that can influence the adsorption of inorganic pollutants in solution.

3.2. Mineralogical Characterization

3.2.1. X-Ray Diffraction (XRD)

Figure 4 shows the XRD pattern. The major mineral phases of the two laterite samples KN and LA include quartz (SiO_2), kaolinite ($Al_2Si_2O_5(OH)_4$), hematite (Fe_2O_3), and goethite (FeO(OH)). These mineral phases are commonly found in laterites [13,34]. The minerals present in KN and LA laterites were compared with other laterites presented in the literature and used for the adsorption of heavy metals and/or metalloids (Table 3).



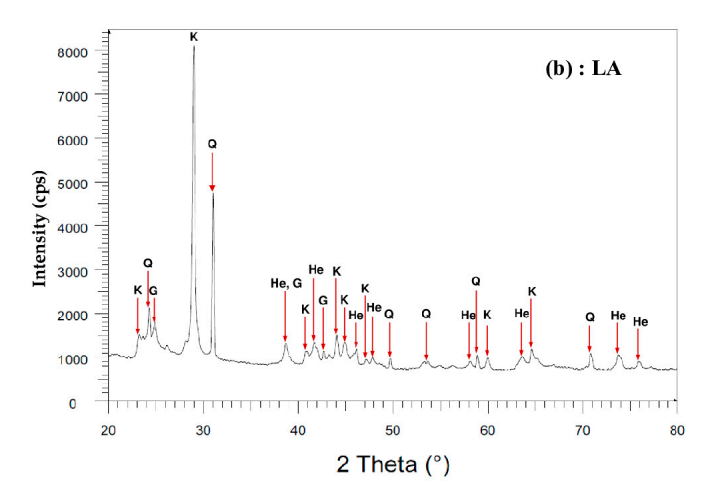


Figure 4. X-ray diffraction pattern of laterite samples: (a) KN sample; (b) LA sample. K = kaolinite; Q = quartz; H = hematite; G = goethite.

Table 3. Comparison of main minerals present in KN and LA laterites with other natural laterites reported in literature.

Samples	Main Minerals	
red soil	quartz, hematite, goethite, aluminum oxides	[35]
raw laterite	quartz, hematite, goethite, aluminum oxides, iron oxides, titanium oxides	[22,36,37]
iron-rich laterite	quartz, hematite, goethite, aluminum oxides	[38]
laterite (Australia)	quartz, hematite, goethite, aluminum oxides	[39]
DA	quartz, hematite, goethite, aluminum oxides	[2]
laterite KN laterite LA	quartz, hematite, goethite, aluminum oxides quartz, hematite, goethite, aluminum oxides	This study

Several authors [8,24–26], who have used laterites to adsorb inorganic pollutants, suggested that these laterites should be rich mainly in hematite, goethite, or aluminum oxides.

3.2.2. Semi-Quantification

Table 4 shows the results of the semi-quantitative analysis of the different mineral phases present in the KN and LA laterites. These results show that the laterites are composed of hematite (13.36% to 11.43%), goethite (7.44% to 6.31%), kaolinite (35.64% to 17.05%), and quartz (33.58% to 45.77%).

Table 4. Mineralogical composition of laterites in % by mass.

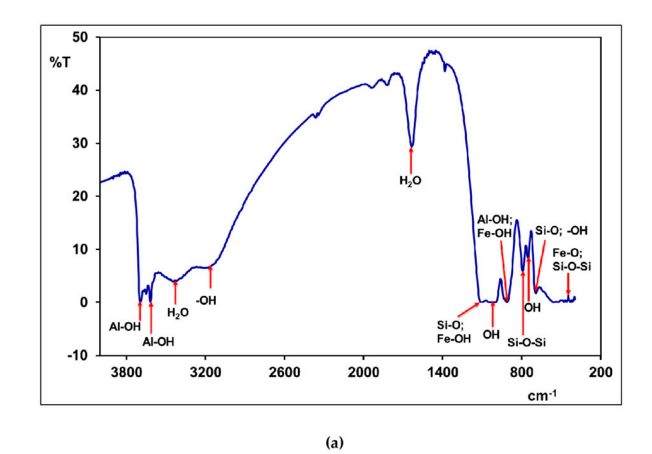
Mineral	Phases	Hematite	Goethite	Kaolinite	Quartz
	KN	13.36	7.44	35.64	33.58
wt (%)	LA	11.43	6.31	17.05	45.77
	DA *	13.11	7.29	48.32	22.53

^{*} DA: previous work on natural laterite (See Reference [2]).

The results from the chemical, mineralogical, cation exchange capacity, and anionic exchange capacity analyses led to the conclusion that the natural laterites investigated possess good adsorbent characteristics for removing inorganic and organic pollutants from aqueous matrices.

3.2.3. Infrared Spectrometry (IR)

Figure 5 shows the FT-IR spectra of the laterite samples. The FT-IR spectra results distinguish three spectral domains: $3700-3400 \text{ cm}^{-1}$, $1650-900 \text{ cm}^{-1}$, and $800-400 \text{ cm}^{-1}$, respectively. Table 5 gives the different attributions of the observed bands.



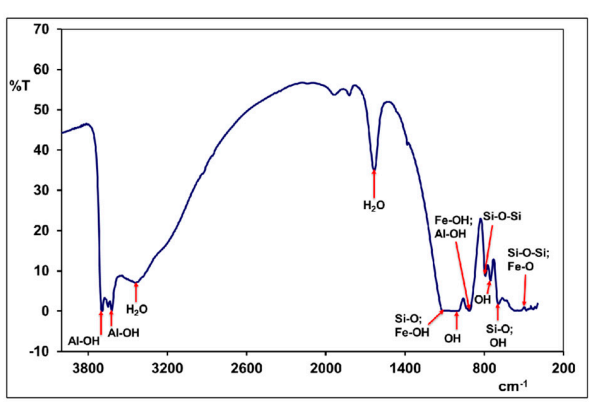


Figure 5. FT-IR spectrum of natural laterites: (a) KN sample; (b) LA sample.

h)

Table 5. Assignments of l	FT-IR bands of KN and	LA laterite samples.

$(\nu \text{ en cm}^{-1})$	Probable Bands Assignments	References
3695	Vibration bands linked to external hydroxyls (Al-OH) in kaolinite	[40]
3618	Vibration bands related to internal hydroxyls (Al-OH) in kaolinite, located between a tetrahedron sheet and an octahedron Al ₂ (OH) ₆	[40]
3170	Band related to –OH bound vibrations in goethite	[41]
3430	Band related to water contained in the intersheet	[40]
1638	Band related to hygroscopic water	[41,42]
1112	Vibration band corresponding to Si-O bound of kaolinite	[40,43,44]
1034	Vibrations bands corresponding to Si-O bound of kaolinite and Fe-OH bound of goethite	[40,44,45]
1004	Vibrations bands related to OH bounds of kaolinite and Fe-OH bound of goethite	[44,45]
914	Band related to distortion vibrations of Al-OH bound of kaolinite and Fe-OH bound of goethite	[40,44,45]
<i>7</i> 91	Band corresponding to bending vibration of Si-O and Fe-OH bounds of kaolinite	[41,43]
752	Vibrations bands related to OH bounds of kaolinite and Fe-OH bound of goethite	[40,45]
694	Vibrations bands related to OH bound of kaolinite and Si-O bounds of quartz	[41]
539	Bands corresponding to distortions vibrations of Si-O-Al bound of kaolinite and Fe-O bound of hematite	[40,41,44]
470	Vibrations bands related to flexion of Si-O-Si and Fe-O bounds of hematite	[41,43]
421	Vibrations bands of Si-O-Si bounds of kaolinite	[44]

The results of the infrared spectrum analysis confirm the presence of mineral phases, such as goethite, hematite, quartz, and kaolinite, which we had already identified during the previous X-ray diffractogram analysis.

3.3. Thermogravimetric Analysis and Differential Scanning Calorimetry (TGA /DSC)

DSC/TGA techniques provide information on the thermal stability and phase transformations of lateritic materials. Figure 6 shows experimental TGA/DSC curves of the KN and LA samples. Several thermal processes are observed. The endothermic peak located between 94 °C and 110 °C in the DSC curves is related to hygroscopic water loss or hydration in the samples. This incident is associated with 1% and 1.5% weight loss in the TGA curves for the KN and LA samples, respectively. Endothermic peaks between 296 °C and 356 °C, followed by 4.1% and 1.3% weight losses for KN and LA, respectively, are due to goethite transformation in hematite (Equation (9)).

$$2\alpha - \text{FeOOH} \longrightarrow \alpha - \text{Fe}_2\text{O}_3 + \text{H}_2\text{O} \tag{9}$$

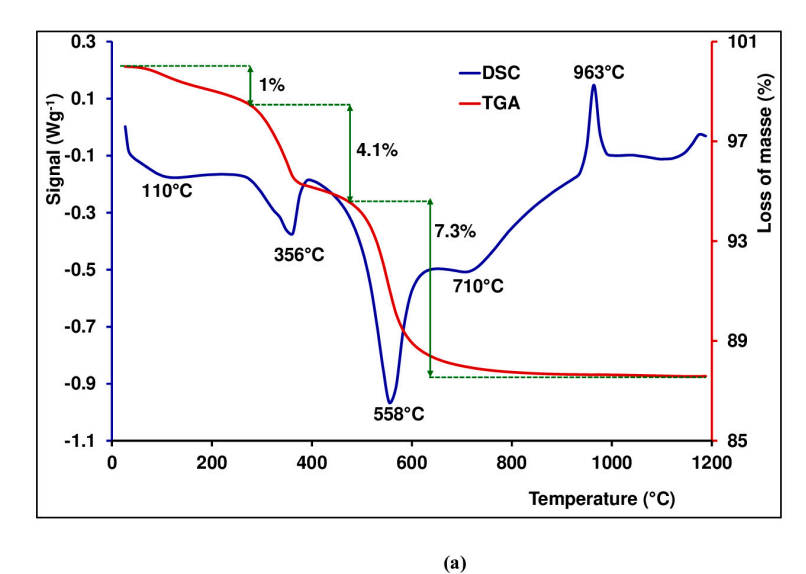
Endothermic peaks between 500 °C and 600 °C in the DSC curves are assigned to kaolinite deshydroxylation (Equation (10)), indicating 7.3% and 8.7% weight losses in the TGA curves for KN and LA, respectively. It is suggested that structural hydroxyls are removed during the chemical reaction, leading to the destruction of the mineral crystalline network. As for kaolinite, deshydroxylation forms an amorphous phase which is named metakaolinite [46,47].

$$Si_2O_5Al_2(OH)_4 \rightarrow 2SiO_2 - Al_2O_3 + 2H_2O$$
 (10)

The only exothermal peaks observed in the DSC curves are located between 950 $^{\circ}$ C and 1000 $^{\circ}$ C. These peaks may be attributed to the structural reorganization of meta kaolinite in the spinel phase and amorphous silica (Equation (11)) [40,46].

$$2[2SiO_2 - Al_2O_3] \rightarrow Si_3Al_4O_{12} + SiO_2$$
 (11)

The DSC/TGA results can indicate changes in the pore structure, influencing the available adsorption sites. DSC analyses reveal the stability of the mineral phases present in laterites. A stable phase is generally more effective at adsorbing anionic and/or cationic pollutants. Temperature variations can affect interactions between laterites and adsorbed molecules. DSC and TGA are essential for understanding the physical and chemical properties of materials, which may include their ability to adsorb contaminants such as heavy metals.



328°C 102 -0.2 110°C Loss of masse Signal (Wg⁻¹) 1.5% 98 -TGA 964°C 94 -DSC 8.7% -1 559°C 90 -1.4 86 200 400 600 800 1000 Temperature (°C) (b)

Figure 6. TGA/DSC curves of lateritic samples: (a) KN sample; (b) LA sample.

3.4. Specific Surface Area and Porosity Using Nitrogen Sorption Analysis

Figure 7 shows the N_2 adsorption–desorption isotherms of the raw laterite samples. The initial part of the isotherms for all laterites of a type I shape (IUPAC classification) indicates the presence of micro pores [48]. As determined by the B.E.T method from Figure 7, the specific surface values are $58.65 \text{ m}^2/\text{g}$ and $41.15 \text{ m}^2/\text{g}$ for the KN and LA samples, respectively. These specific surface area values are significantly high when compared to values reported in the literature for natural laterites in the range of $16–32 \text{ m}^2/\text{g}$ [15,17,22,36–38] (Table 6).

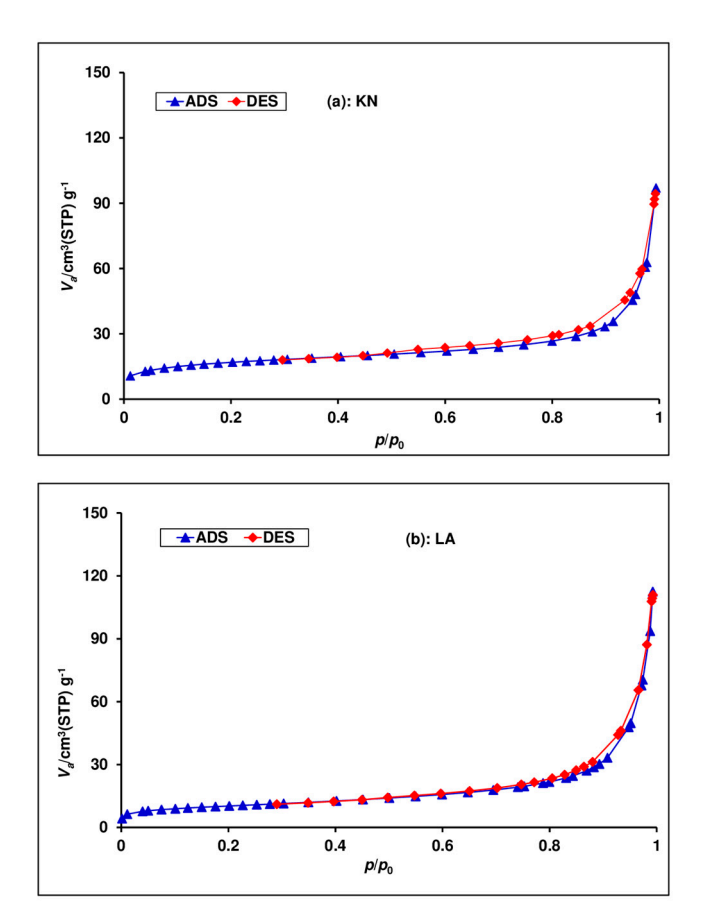


Figure 7. N₂ adsorption/desorption isotherms of (a) KN and (b) LA.

Table 6. Specific surface area B.E.T values, pore volume of two samples, and literature-reported specific areas of other laterites.

Laterites	Specific Surface Area Pore Volum by B.E.T (m²/g) (cm³/g)		References
Laterite raw (India)	15.3	0.013	[15]
Red soil	16.1	-	[35]
Laterite raw (India)	17.5–18.5	0.011	[36]
Modified laterite	178–184	0.22	[36]
Laterite raw (Vietnam)	10.9	0.01	[49]
Laterite raw	24.7	0.08	[37]
Iron rich laterite	32	-	[38]
Calcined laterite	187.5	0.04	[50]
Laterite soil (DA)	35.08	0.10	[28]
Laterite soil (KN)	58.6	0.14	This study
Laterite soil (LA)	41.1	0.10	This study

We noted that our investigated lateritic materials showed high specific surface area values compared with most natural materials reported in the literature used to remove inorganic pollutants. These particular surface areas suggest that the natural materials we investigated are potential candidates for the adsorption of inorganic pollutants in solution. Several authors have highlighted the importance of having high specific surface area values in their studies using clay and/or lateritic materials to remove inorganic pollutants [50,51].

3.5. Determination of Anionic Exchange Capacity (AEC)

The anionic exchange capacity values (Table 7) of the measured laterites ranged from 86.50 ± 3.40 to 73.91 ± 9.94 cmol(-)·kg⁻¹ and 73.59 ± 3.02 to 64.56 ± 4.08 cmol(-)·kg⁻¹,

Minerals **2025**, 15, 379 15 of 24

respectively. The anionic exchange capacity of laterites increased with the decreasing pH of the solution. This significant increase in AEC with decreasing pH is due to positive charges that are located on iron hydroxides associated with aluminum. The high values of the anionic exchange capacities of the investigated laterites would be an asset for using them as adsorbents to remove anionic pollutants.

Table 7. Anionic exchange of	capacity of laterites.
-------------------------------------	------------------------

Laterite KN		Lat	erite LA
рН	AEC (cmol(-)·kg ⁻¹)	рН	AEC (cmol(-)·kg ⁻¹)
3.47 ± 0.02	6.50 ± 3.40	3.67 ± 0.04	73.59 ± 3.02
3.67 ± 0.01	86.02 ± 8.29	3.84 ± 0.04	73.33 ± 3.03
5.51 ± 0.05	73.91 ± 9.94	5.22 ± 0.04	64.56 ± 4.08

The results obtained are similar to other materials studied in the literature. Cheng et al. determined the anionic exchange capacity of black carbon at pH 7.1 and 3.4 and obtained values of 84 and 18 cmol·kg⁻¹, respectively [52]. Lawrinenko et al. also determined the anionic exchange capacity of biochar produced from three raw materials at 500 and 700 °C at pH 4, 6, and 8 [53]. The measured AEC values ranged from 0.60 to 27.8 cmol(-)·kg⁻¹. Moreover, the study by Schell and Jordan [54], on kaolinite, pyrophyllite, halloysite, and bentonite materials showed that there are close relationships between the anionic exchange capacity of these materials and their physicochemical properties. Indeed, materials rich in iron oxide, aluminum oxide, and amorphous silicates showed a high anionic exchange capacity. Consequently, the investigated natural laterites containing important amounts of iron oxide and alumina are likely to exhibit high anionic exchange capacity values, which gives them interesting adsorbent properties.

3.6. Determination of Cation Exchange Capacity (CEC)

The CEC value, determined using the hexaamminecobalt (III) chloride method, is an important parameter in assessing the adsorption capacity of adsorbent materials for cations removal [18]. We found high CEC values in the order of 52.3 ± 2.3 and 58.7 ± 3.4 cmol(+)/kg (dried matter) for the KN and LA samples, respectively. We cannot compare these results with previous literature data because we did not find extensive documentation of this parameter for natural laterites that remove inorganic pollutants from solution. To our knowledge, this study appears to be the first to provide scientific documentation of this parameter for laterites used in the field of adsorption of inorganic pollutants. However, we compare the CEC values obtained in this study with other adsorbents in Table 8 below. These specific surface area values are significantly high when compared to values reported in the literature for other natural laterites. We noted that the CEC values of the KN and LA laterite samples are comparable with those reported for other natural adsorbents. Considering the CEC and the specific surface area values, compared with the literature values on natural adsorbents, these materials could be considered potential candidates for heavy metal cation removals through adsorption processes [55,56].

The laterites of Burkina are rich in iron oxide and alumina, like the laterites of other countries used to eliminate heavy metals and/or metalloids in ground waters [36,37,57]. Considering all of these physical and chemical characteristics, we can conclude that the natural laterites of Burkina Faso prove to be potential candidates for the adsorption of heavy metals and/or metalloids in groundwater.

Adsorbents	C.E.C (cmol(+)/kg)	References
Clay mineral	42.38	[58]
Peat soil	33–48	[59]
Bauxite	24–33	[59]
Iron concretion	59–65	[59]
Natural clay	18.66	[60]
Kaolinite	13.00	[61]
Bentonitic clay	67.00	[62]
Ivory Coast clay	35.47	[63]
Laterite soil (KN)	52.33	This study
Laterite soil (LA)	58.70	This study

Table 8. Comparison of CEC values for KN and LA laterites with other adsorbents.

3.7. Isoelectric Point (IP) of Laterite Samples

Figure 8 shows variations in the zeta potential versus pH of the laterite sample solutions. These variations allowed the determination of isoelectric points (IP). For zeta potentials whose values equal zero, the IP values are 3.82 and 3.78 for the KN and LA samples, respectively. According to the literature [64], the theoretical value of IP, calculated based on the silica and alumina percentage, is approximatively 4.6. The experimental values of IP are not far from the theoretical value. The observed deviations are the result of the iron percentage being higher than the one of alumina and also by the presence of other oxides in the samples.

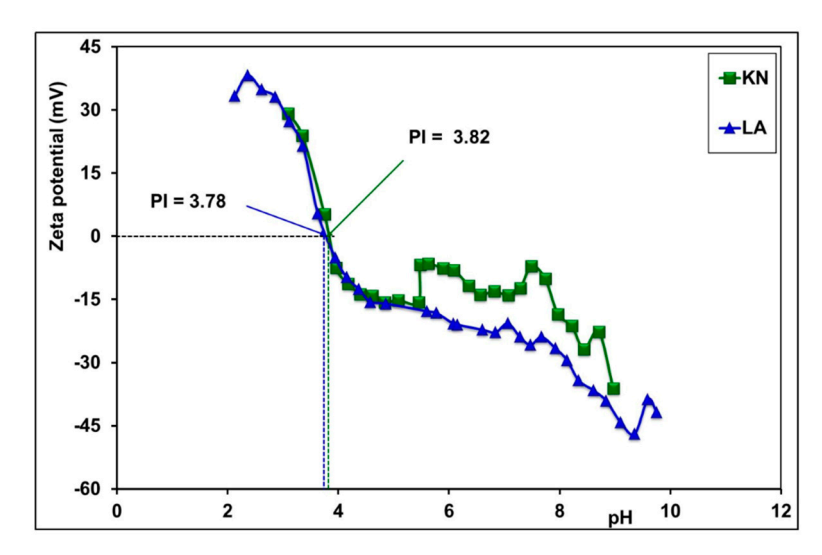


Figure 8. Isoelectric point of laterite soils determined from variations in zeta potential versus pH.

The values of the isoelectric point (IP) of laterites, KN (3.82) and LA (3.78), mean that the surfaces of these laterites are positively charged at pH levels below these values, which favors the adsorption of anionic pollutants. The increase in adsorption below IP is due to electrostatic attraction between the positive surface and the negative charge of the anions. Similarly, the decrease in adsorption with increasing pH is due to electrostatic repulsion between the opposing surface and the negative charge of anions. The electric surface charge plays an important role in the adsorption of inorganic pollutants on laterites.

3.8. Batch Adsorption Experiments: Application to Arsenic (III, V) and Pb(II) and Cu(II) Removal

Figure 9a shows the removal percentage of As(III, V) versus adsorbent doses, at a concentration of 5 mg/L and at a pH varying between 6.57 and 7.15 and 6.5–7 for As(V) and As(III), respectively. An increase in adsorbent dose from 2.5 to 15 g/L leads to arsenic (III)

removal efficiency from 80% to 98% for LA and KN samples, respectively. As for arsenic (V), the removal efficiency is 99% for both adsorbents KN and LA samples.

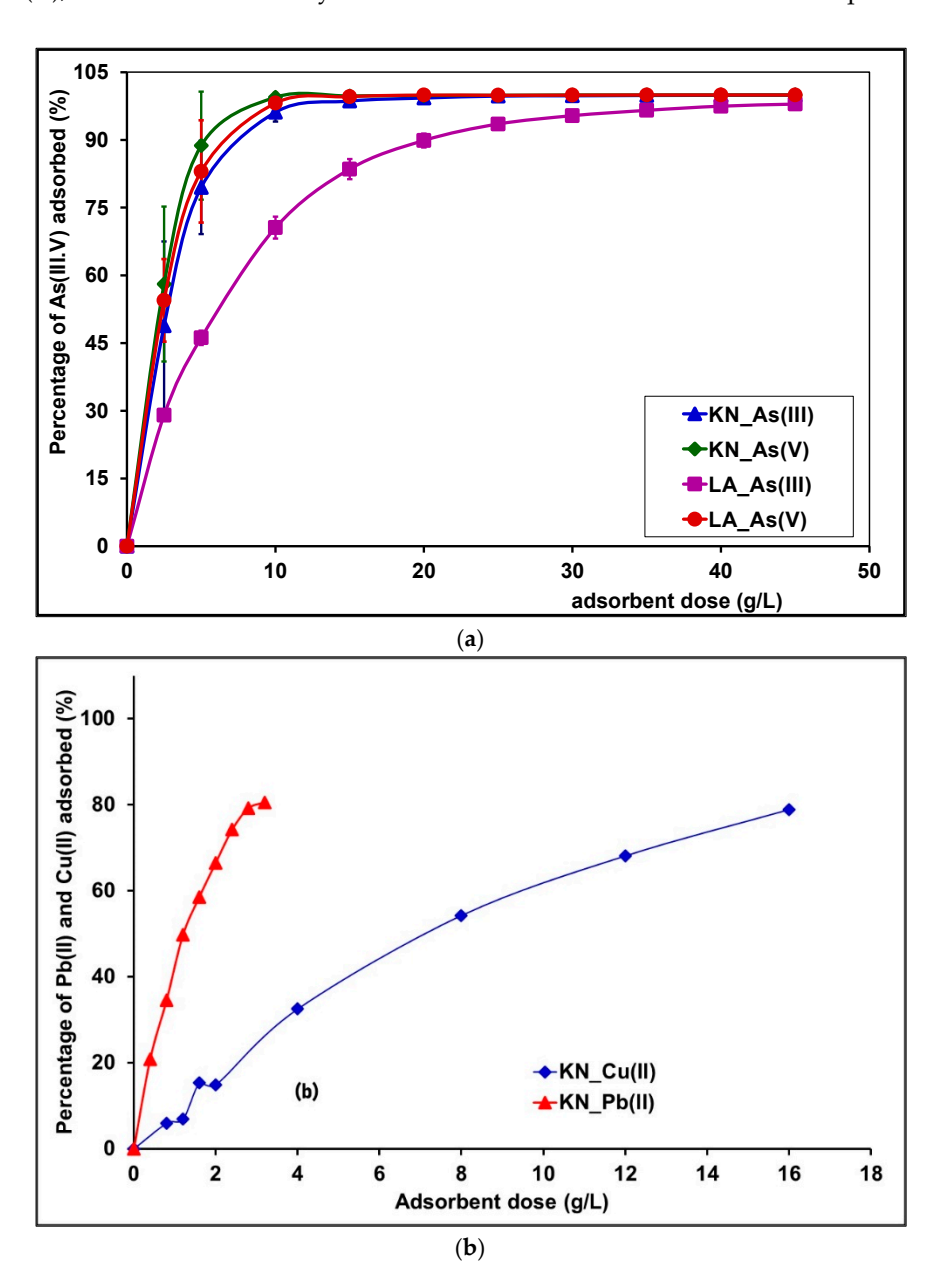


Figure 9. (a) Effect of adsorbent dose on adsorption of As(III, V). (b) Effect of KN adsorbent dose on adsorption of Pb(II) and Cu(II).

With an amount of 15 g/L of the laterites from Burkina Faso, As(III) removal percentages, reaching 98% and 80%, are achieved for the laterites KN and LA, respectively, with an initial arsenite concentration of 5 mg/L. With an initial arsenite concentration of 1 mg/L, Pravin D. Nemade et al. obtained a rate of elimination of 90% for an amount of 25 g laterite/L [36]. With an amount of 15 g/L of the KN and LA samples and an initial arsenate concentration of 5 mg/L, a removal rate of As(V) of more than 95% was achieved. The results in the present work are better than those obtained by Abhijit Maiti et al. on a natural laterite coming from the zone of Midnapore of Western Bengal (India) for which a removal rate of approximately 80% was achieved when using 15 g laterite/L [22]. For an amount of 5 g/L, a removal rate of approximately 70% is achieved for both KN and LA laterites of Burkina in the case of As(V) adsorption (initial arsenate concentration of 5 mg/L), and a removal rate of approximately 80% for laterite KN in the case of As(III)

adsorption (initial arsenite concentration of 5 mg/L). Trivalent arsenic (As(III)) is less adsorbed on LA laterite than on KN laterite for the following reasons. KN laterite has a higher proportion of iron oxides (20.8%) and aluminum (14.09%), providing more adsorption sites for As(III) and promoting stronger interactions. Additionally, KN laterite's specific surface area (58.6 m 2 /g) and porosity (0.14 cm 3 /g) exceed those of LA laterite, which are 41.1 m 2 /g and 0.10 cm 3 /g, respectively, allowing better accessibility for As(III) adsorption. Finally, KN laterite's anionic exchange capacity is also higher than that of the LA laterite in the studied pH range, further enhancing its effectiveness as an adsorbent for arsenic.

The efficiency of the removal may be due to an increase in adsorption sites which are made available when the dosage of adsorbent dose increases [65]. For both the KN and LA samples, a high removal percentage is achieved with an amount of natural laterites, which is lesser than those described in the literature. This result could be attributed to the high specific area and anionic exchange capacity of the laterites KN and LA of Burkina Faso. These results are in agreement with the literature data showing that better results are achieved when using adsorbents with large specific surface area [36]. However, contrary to the previous reported literature, the present work shows that the specific surface area must be combined to the anionic exchange capacity for a better interpretation.

The results for the removal of Pb(II) and Cu(II) metal ions at different doses of adsorbent are presented in Figure 9b. A general trend observed was that the adsorption of heavy metal ions increased with the increase in adsorbent dose. The results show that the removal rates of Pb(II) reached $74.20 \pm 0.95\%$ (3.09 ± 0.04 mg/g) when the amount of the KN adsorbent was 2.4 g/L. For Cu(II), the adsorption rates were $54.18 \pm 0.01\%$ (0.68 ± 0.01 mg/g) when the dose of the KN adsorbent was 8 g/L. As the dose of laterite increased, the removal of Pb(II) and Cu(II) from the solutions also increased. This can be explained by the increase in functional groups on the surface of the laterite, providing a greater number of available sites to form complexes through surface complexation, or to exchange cations due to the ion exchange process [66-68].

Arsenic is better adsorbed on laterites than copper and lead due to its stronger chemical affinity for the adsorption sites present on laterites, such as iron and aluminum oxides, which promote specific interactions. Additionally, the size and charge of arsenic allow it to be attached more effectively to these surfaces compared to copper and lead ions.

3.9. A Comparison of the Main Physicochemical Properties Related to the Adsorption of Laterites from Burkina Faso with Those Reported in the Literature

This study investigated the main physicochemical properties of two laterites (LA and KN) from Burkina Faso, showing how to link these properties to an adsorption process. The results showed that these laterites possess interesting properties, allowing them to be used to treat water contaminated by anionic and/or cationic pollutants. The physicochemical properties of the two laterites with regard to their adsorption properties were compared with other results reported in the literature concerning laterites used for the adsorption of anionic and/or cationic pollutants. Table 9 shows the main observations of this comparison. From the results of Table 9, we noted that the CEC and AEC determinations of lateritic materials are omitted in most studies dealing with the removal of cationic and/or anionic pollutants from aqueous solutions. However, these parameters are crucial to elucidate the adsorption mechanisms, in terms, for example, of surface complexation (inner-sphere and outer-sphere surface complexation). While CEC value is an important parameter to determine the adsorption of heavy metal cations, AEC values are more indicated for adsorbents like As(III) and As(V), which appear in solution as neutral or anionic-charged species.

Table 9. Comparison of physicochemical properties of several lateri	tes in relation to pollutant
adsorption.	

Adsorbent	Adsorbats	AEC cmol(-)/kg)	C.E.C cmol(+)/kg)	Specific Surface Area (B.E.T) (m²/g)	Pore Volume (cm³/g)	DSC /TGA	IEP or PZC	References
Laterite soil	cationic dye	-	-	66.97	-	-	6.6	[69]
Raw laterite	arsenic and fluoride	-	-	31.6037	0.0097	-	-	[70]
Raw laterite	Phosphate	-	-	29.54	0.0676	-	-	[7]
Laterite	Arsenic	-	-	155	0.5489	-	7.1	[8]
Laterite clay	Ni(II) and Co(II)	-	-	17.441	0.005	-	-	[23]
Laterite soil	Arsenic	-	-	15.365	0.013	-	6.96	[15]
Natural laterite	Arsenic	-	-	18.05	-	-	7.49	[16]
Treated laterite	Led	-	-	75.5	0.02	-	6.0	[71]
Plateau laterite ceramic	Pb, Cd, Hg, As, Cu and Cr	-	-	26.73	0.15	-	-	[27]
Limonitic laterite	Pb(II) and Cd(II)	-	-	62.73	0.62	-	-	[24]
Lateritic nickel	Pb(II)	-	-	68.39	-	-	6.70	[26]
Laterite soil	Pb(II) and Cr(VI)	-	-	23.015	0.011	-	-	[25]
Laterite DA **	As(III,V)	40.61- 230.80	-	35.08	0.10	-	4.75	[2,28]
Laterite LA *	As(III,V)	64.56-73.59	58.7 ± 3.4	58.80	0.14	Det ***	3.78	This study
Laterite KN *	As(III,V)	73.90-86.50	52.3 ± 2.3	41.10	0.10	Det **	3.82	This study

^{*} Composition mineralogical characterization of laterites are common characteristics provided in most studies (see Table 3). ** References [2,28] describe our previous study on a natural laterite; Det ***: determined.

Table 9 shows that our study is the first to provide a complete description of laterite properties, in terms of specific surface area, pore volume, DSC/TGA, PZC, chemical composition*, mineralogical characterization*, cation exchange capacity (CEC), and anionic exchange capacity (AEC), in relation to the adsorption ability of the material. Indeed, these properties are helpful criteria that provide strong evidence of the adsorption capacity of the laterites regarding the removal of cationic and/or anionic pollutants from aqueous solutions [18–20,54].

It is worth noting that the adsorptive properties of laterites are closely related to the geology of the deposit ore they originate from. Indeed, for a naturally occurring laterite ore, the type of parent rock it originates from determines its chemical composition, particularly the percentages of iron, aluminum, silica, and titanium oxides, as well as its mineralogical composition. The mineralogical composition is generally characterized by mineral phases such as goethite, hematite, and kaolinite. However, laterite ores possess a large variability in their composition. Consequently, even if different geological environments are qualitatively characterized by the same chemical and mineralogical composition, the percentage of oxides can be different from one site to another. The physicochemical properties may also vary. In these circumstances, it is appropriate to focus on quantitative criteria that we need to forecast the ability of the material to remove pollutants in the adsorption process. Moreover, the extent of these criteria may lead to different adsorption capacities. As we have already stated, these critical criteria are the following: specific surface area, pore volume, PZC or IEP, cation exchange capacity (CEC), and anionic exchange capacity (AEC).

The laterites LA and KN in this study are from two sites of different geological environments (Table 10). The first site is an environment of Birimian rocks, resulting from the weathering of andesite (with a calcic-alkaline affinity), basalt, and dacit. On the other hand, the second site is a weathering site of alkaline granites located in a Precambrian rock environment. Preliminary investigations showed (Table 10) that the removal percentage for arsenic (III) removal at a concentration of 5 mg/L and an adsorbent dose of 15 g/L leads to arsenic (III) removal of $80 \pm 0.15\%$ and $98 \pm 0.05\%$ for the LA and KN

Minerals **2025**, 15, 379 20 of 24

samples, respectively [72]. As for arsenic (V), the removal efficiency was $99 \pm 0.02\%$ for the two samples, KN and LA, at an adsorbent dose of 15 g/L [72]. Although the two laterites (LA and KN) do not have the same geological environments, they showed a high efficiency for arsenic removal due to the combination of their AEC, specific surface area, and pore volume values. In addition, their low IEP or PZC values also favored the adsorption of neutral or anionic-charged arsenic species. Adsorption of anionic arsenic species will only be important when the charges on the laterites become positive, which happens at low soil solution pH where anionic-charged arsenic species occur [2,28]. Noting that the surfaces of the samples are positively charged under their PZC values, it is clear these materials better adsorb arsenate (V) anions at pH values under their PZC values. It is, therefore, important to measure the anionic exchange capacity (AEC) of the laterites rather than the CEC when we are dealing with the adsorption of neutral or anionic-charged arsenic species.

Table 10. Adsorptive properties of laterites used for As(III, V) removal in relation to their physicochemical characteristics.

Laterite	Geological Environment	Mineralogical Characterizations XRD, FT-IR	AEC cmol(-)/kg)	Specific Surface Area (B.E.T) (m ² /g)	Pore Volume (cm³/g)	IEP or PZC	Efficiency (%)
KN	Environment of Birimian rocks, resulting from the weathering of andesite (with a calcic-alkaline affinity), basalt, and dacit	Det *	73.90–86.50	58.80	0.14	3.82	98 ± 0.05% for As(III) 99 ± 0.02% for As(V)
LA	Environment of precambrian rocks and alteration of alkaline granites	Det *	64.56–73.59	41.10	0.10	3.78	$80 \pm 0.15\%$ for As(III) $99 \pm 0.02\%$ for As(V)
DA	Lateritic plateau, well indurated and resulting from the alteration of a neutral basic rock	Det *	40.61–230.80	35.08	0.10	4.75	99.69% for As(V)) 97.30% for As(III)

Det *: determined (Tables 3 and 5).

At this step, the geological environment cannot constitute the sole criterion that would justify the adsorption capacity of negatively charged arsenic species. This criterion may not be decisive in predicting the adsorption capacity of laterite. It must be associated with the physicochemical properties of the laterites. Table 10 outlines the criteria that affect the adsorptive properties of laterites (LA, KN) in connection with their physicochemical and geological characteristics.

To date, it has been demonstrated that when particular geological environments, such as Birimian/Precambrian and lateritic plateaus, are combined with appropriate physicochemical properties, a potential lateritic material for adsorption is expected (Table 10). Unfortunately, in the literature, no direct link has yet been established on this subject. This study constitutes a preliminary finding, which we will validate by extending our investigations to other lateritic sites in Burkina Faso.

4. Conclusions

Physicochemical and mineralogical analyses were carried out on two natural laterites from the country. The properties of these two natural laterites were determined with regard to their ability to adsorb heavy metals and/or metalloids from aqueous solutions. These laterite samples were characterized using several physical and chemical techniques, including XRD, FTIR, elementary chemical analyses, and SEM. The results obtained by

Minerals **2025**, 15, 379 21 of 24

X-ray diffraction analysis coupled with infrared showed that the laterites are composed of hematite (13.36% to 11.43%), goethite (7.44% to 6.31%), kaolinite (35.64% to 17.05%), and quartz (33.58% to 45.77%). Chemical analysis showed that these natural laterites are rich in iron and aluminum oxide. The specific surface areas and cation exchange capacity values, as determined by the BET and cobalt hexamine chloride methods, were shown to have suitable values compared to previously determined values in the literature. The anionic exchange capacity of laterites KN and LA ranged from 86.50 ± 3.40 to 73.91 ± 9.94 cmol(-)·kg⁻¹ and from 73.59 \pm 3.02 to 64.56 \pm 4.08 cmol(-)·kg⁻¹, respectively. Furthermore, the investigations on these laterite samples showed that they could remove heavy metals and/or metalloids from contaminated ground waters. The main minerals identified in these two Burkina Faso laterities were consistent with those described in the literature. This study led to some valuable criteria we can use as a basis for classifying natural laterites as potential adsorbent materials for the removal of inorganic and/or organic pollutants from aqueous matrices. At a dose of 15 g/L, the elimination of arsenic (III) is 80% for sample LA and 98% for sample KN, while the elimination efficiency of arsenic (V) reaches 99% for both samples. Regarding Pb(II), the elimination rate with 2.4 g/L of KN adsorbent is $74.20 \pm 0.95\%$ $(3.09 \pm 0.04 \text{ mg/g})$, and for Cu(II), it is $54.18 \pm 0.01\%$ ($0.68 \pm 0.01 \text{ mg/g}$) with 8 g/L of KN adsorbent. The adsorption of As(III,V), Pb(II), and Cu(II) species on the surfaces of laterites would primarily occur through the formation of surface complexes, which can be either inner-sphere or outer-sphere complexes. This study showed how the geological environment determined the mineralogical characteristics of the laterites and their chemical composition. Combining the geological environment with appropriate criteria related to the physicochemical properties of the materials opens up interesting perspectives regarding the rapid valorization of the laterites in Burkina Faso as potential adsorbents. To deepen the understanding of the adsorption mechanisms, detailed studies will be conducted using various techniques to reduce the uncertainty associated with the hypotheses regarding the nature of the formed complexes. Additionally, the analysis of the FTIR spectra of the residues will help to identify the chemical modifications that occur during adsorption, thereby providing crucial information on the interactions between the metals and the lateritic surfaces.

Author Contributions: Conceptualization, C.B., A.-L.H., and B.G.; methodology, C.B., L.C. and A.-L.H.; software, C.B.; validation, C.B. and L.C.; formal analysis, C.B.; investigation, C.B.; resources, L.C., A.-L.H., and B.G.; data curation, C.B., L.C.; A.-L.H., and B.G.; writing—original draft preparation, C.B.; writing—review and editing, C.B., L.C., A.-L.H., and B.G.; visualization, C.B. and A.-L.H.; supervision, B.G. and A.-L.H.; project administration; A.-L.H. and B.G.; funding acquisition, B.G. and A.-L.H. All authors have read and agreed to the published version of the manuscript.

Funding: The authors thank the ARES-CCD/PIC 2012 (Belgium) and the International Science Program (ISP, Uppsala, Sweden, BUF 02) for providing financial support.

Data Availability Statement: All data generated or analyzed during this study are included in this published article.

Acknowledgments: The authors thank the following services for their assistance: the departments of materials science, of metallurgy, and of thermodynamic and physical mathematics of UMONS and Materia Nova Research Center (Belgium).

Conflicts of Interest: The authors declare no conflicts of interest regarding the publication of this paper.

References

1. Ndiaye, M.; Magnan, J.P.; Cissé, I.K.; Cissé, L. Étude de l'amélioration de latérites du Sénégal par ajout de sable. *Bull. Lab. Ponts Chaussees* **2013**, *280*, 123–137.

Minerals **2025**, 15, 379 22 of 24

2. Ouedraogo, R.D.; Bakouan, C.; Sorgho, B.; Guel, B.; Bonou, L.D. Characterization of a natural laterite of Burkina Faso for the elimination of arsenic (III) and arsenic (V) in groundwater. *Int. J. Biol. Chem. Sci.* **2019**, *13*, 2959–2977. [CrossRef]

- 3. Najar, M.; Sakhare, V.; Karn, A.; Chaddha, M.; Agnihotri, A. A study on the impact of material synergy in geopolymer adobe: Emphasis on utilizing overburden laterite of aluminium industry. *Open Ceram.* **2021**, 7, 100163. [CrossRef]
- 4. Lawane, A.; Pantet, A.; Vinai, R.; Hugues, J. Etude géologique et géomécanique des latérites de Dano (Burkina Faso) pour une utilisation dans l'habitat, XXIXe Recontres Univ. *Genie Civ.* **2011**, *86*, 206–215.
- 5. Bourman, R.P.; Ollier, C.D. A critique of the Schellmann definition and classification of laterite. Catena 2002, 47, 117–131. [CrossRef]
- 6. Maiti, A.; Thakur, B.K.; Basu, J.K.; De, S. Comparison of treated laterite as arsenic adsorbent from different locations and performance of best filter under field conditions. *J. Hazard. Mater.* **2013**, 262, 1176–1186. [CrossRef] [PubMed]
- 7. Huang, W.Y.; Zhu, R.H.; He, F.; Li, D.; Zhu, Y.; Zhang, Y.M. Enhanced phosphate removal from aqueous solution by ferric-modified laterites: Equilibrium, kinetics and thermodynamic studies. *Chem. Eng. J.* **2013**, 228, 679–687. [CrossRef]
- 8. Nguyen, T.H.; Tran, H.N.; Vu, H.A.; Trinh, M.V.; Nguyen, T.V.; Loganathan, P.; Vigneswaran, S.; Nguyen, T.M.; Trinh, V.T.; Vu, D.L.; et al. Laterite as a low-cost adsorbent in a sustainable decentralized filtration system to remove arsenic from groundwater in Vietnam. *Sci. Total Environ.* **2020**, 699, 134267. [CrossRef]
- 9. Nguyena, T.H.; Nguyen, A.T.; Loganathan, P.; Nguyen, T.V.; Vigneswaran, S.; Nguyen, T.H.H.; Trand, H.N. Low-cost laterite-laden household filters for removing arsenic from groundwater in Vietnam and waste management. *Process Saf. Environ. Prot.* **2021**, 152, 154–163. [CrossRef]
- 10. Thanakunpaisit, N.; Jantarachat, N.; Onthong, U. Removal of Hydrogen Sulfide from Biogas using Laterite Materials as an Adsorbent. *Energy Procedia* **2017**, *138*, 1134–1139. [CrossRef]
- 11. Kamagate, M.; Assadi, A.A.; Kone, T.; Giraudet, S.; Coulibaly, L.; Hanna, K. Use of laterite as a sustainable catalyst for removal of fluoroquinolone antibiotics from contaminated water. *Chemosphere* **2018**, *195*, 847–853. [CrossRef] [PubMed]
- 12. Karki, S.; Timalsina, H.; Budhathoki, S.; Budhathoki, S. Arsenic removal from groundwater using acid-activated laterite. *Groundw. Sustain. Dev.* **2022**, *18*, 100769. [CrossRef]
- 13. Millogo, Y.; Traoré, K.; Ouedraogo, R.; Kaboré, K.; Blanchart, P.; Thomassin, J.H. Geotechnical, mechanical, chemical and mineralogical characterization of a lateritic gravels of Sapouy (Burkina Faso) used in road construction. *Constr. Build. Mater.* **2008**, 22, 70–76. [CrossRef]
- 14. Lawane, A.; Vinai, R.; Pantet, A.; Thomassin, J.-H.; Messan, A. Hygrothermal Features of Laterite Dimension Stones for Sub-Saharan Residential Building Construction. *J. Mater. Civ. Eng.* **2014**, *26*, 05014002. [CrossRef]
- 15. Maji, S.K.; Pal, A.; Pal, T.; Adak, A. Adsorption Thermodynamics of Arsenic on Laterite Soil. J. Surf. Sci. Technol. 2007, 22, 161–176.
- 16. Maiti, A.; Dasgupta, S.; Basu, J.; De, S. Adsorption of arsenite using natural laterite as adsorbent. *Sep. Purif. Technol.* **2007**, *55*, 350–359. [CrossRef]
- 17. Kadam, A.M.; Nemade, P.D.; Oza, G.H.; Shankar, H.S. Treatment of municipal wastewater using laterite-based constructed soil filter. *Ecol. Eng.* **2009**, *35*, 1051–1061. [CrossRef]
- 18. Xu, D.; Tan, X.L.; Chen, C.L.; Wang, X.K. Adsorption of Pb(II) from aqueous solution to MX-80 bentonite: Effect of pH, ionic strength, foreign ions and temperature. *Appl. Clay Sci.* **2008**, *41*, 37–46. [CrossRef]
- 19. Eren, E.; Afsin, B. An investigation of Cu(II) adsorption by raw and acid-activated bentonite: A combined potentiometric, thermodynamic, XRD, IR, DTA study. *J. Hazard. Mater.* **2008**, *151*, 682–691. [CrossRef]
- Melichová, Z.; Hromada, L. Adsorption of Pb²⁺ and Cu²⁺ Ions from Aqueous Solutions on Natural Bentonite, Polish. J. Environ. Stud. 2012, 22, 457–464.
- 21. Moutou, J.M.; Foutou, P.M.; Matini, L.; Samba, V.B.; Mpissi, Z.F.D.; Loubaki, R. Characterization and Evaluation of the Potential Uses of Mouyondzi Clay. *J. Miner. Mater. Charact. Eng.* **2018**, *06*, 119–138. [CrossRef]
- 22. Maiti, A.; DasGupta, S.; Basu, J.K.; De, S. Batch and Column Study: Adsorption of Arsenate Using Untreated Laterite as Adsorbent. *Ind. Eng. Chem. Res.* **2008**, 47, 1620–1629. [CrossRef]
- Ghani, U.; Hussain, S.; Amin, N.U.; Imtiaz, M.; Khan, S.A. Laterite clay-based geopolymer as a potential adsorbent for the heavy metals removal from aqueous solutions. J. Saudi Chem. Soc. 2020, 24, 874

 –884. [CrossRef]
- 24. He, F.; Ma, B.; Wang, C.; Chen, Y.; Hu, X. Adsorption of Pb(II) and Cd(II) hydrates via inexpensive limonitic laterite: Adsorption characteristics and mechanisms. Sep. *Purif. Technol.* **2023**, *310*, 123234. [CrossRef]
- 25. Mitra, S.; Thakur, L.S.; Rathore, V.K.; Mondal, P. Removal of Pb(II) and Cr(VI) by laterite soil from synthetic waste water: Single and bi-component adsorption approach. *Desalin. Water Treat.* **2016**, *57*, 18406–18416. [CrossRef]
- 26. Mohapatra, M.; Khatun, S.; Anand, S. Kinetics and thermodynamics of lead (II) adsorption on lateritic nickel ores of Indian origin. *Chem. Eng. J.* **2009**, 155, 184–190. [CrossRef]
- 27. Zhu, D.; He, Y.; Zhang, B.; Zhang, N.; Lei, Z.; Zhang, Z.; Chen, G.; Shimizu, K. Simultaneous removal of multiple heavy metals from wastewater by novel plateau laterite ceramic in batch and fixed-bed studies. *J. Environ. Chem. Eng.* **2021**, *9*, 105792. [CrossRef]

Minerals **2025**, 15, 379 23 of 24

28. Ouedraogo, R.D.; Bakouan, C.; Sakira, A.K.; Sorgho, B.; Guel, B.; Somé, T.I.; Hantson, A.L.; Ziemons, E.; Mertens, E.; Hubert, P.; et al. The Removal of As(III) Using a Natural Laterite Fixed-Bed Column Intercalated with Activated Carbon: Solving the Clogging Problem to Achieve Better Performance. *Separations* **2024**, *11*, 129. [CrossRef]

- 29. Koffi, Y.H.; Wenmenga, U.; Djro, S.C. Tarkwaian Deposits of the Birimian Belt of Houndé: Petrological, Structural and Geochemical Study (Burkina-Faso, West Africa). *Int. J. Geosci.* **2016**, *7*, 685–700. [CrossRef]
- 30. Njopwouo, D.; Orliac, M. Note sur le comportement de certains minéraux à l'attaque triacide. *Cah. ORSTOM Sér. Pédol.* **1979**, 17, 329–337.
- 31. Laibi, A.B.; Gomina, M.; Sorgho, B.; Sagbo, E.; Blanchart, P.; Boutouil, M.; Sohounhloule, D.K.C. Caractérisation physico-chimique et géotechnique de deux sites argileux du Bénin en vue de leur valorisation dans l'éco-construction. *Int. J. Biol. Chem. Sci.* **2017**, 11, 499–514. [CrossRef]
- 32. Zelazny, L.W.; He, L. Chapter 41 Charge Analysis of Soils and Anion Exchange. In *Methods of Soil Analysis: Part 3 Chemical Methods—SSSA Book Series*; Sparks, D.L., Page, A.L., Helmke, P.A., Loeppert, R.H., Soltanpour, P.N., Tabatabai, M.A., Johnston, C.T., Sumner, M.E., Eds.; Wiley: Hoboken, NJ, USA, 1996; Volume 5, pp. 1231–1253. [CrossRef]
- 33. Konan, K.L. Interactions Entre des Matériaux Argileux et un Milieu Basique Riche en Calcium. Ph.D. Thesis, Université de Limoge, Limoges, France, 2006; pp. 1–144.
- 34. Mbumbia, L.; De Wilmars, A.M.; Tirlocq, J. Performance characteristics of lateritic soil bricks fired at low temperatures: A case study of Cameroon. *Constr. Build. Mater.* **2000**, *14*, 121–131. [CrossRef]
- 35. Nemade, P.D.; Kadam, A.M.; Shankar, H.S.; Bengal, W. Adsorption of arsenic from aqueous solution on naturally available red soil. *J. Environ. Biol.* **2009**, *30*, 499–504.
- 36. Maiti, A.; Basu, J.K.; De, S. Experimental and kinetic modeling of As(V) and As(III) adsorption on treated laterite using synthetic and contaminated groundwater: Effects of phosphate, silicate and carbonate ions. *Chem. Eng. J.* **2012**, *191*, 1–12. [CrossRef]
- 37. Glocheux, Y.; Pasarín, M.M.; Albadarin, A.B.; Allen, S.J.; Walker, G.M. Removal of arsenic from groundwater by adsorption onto an acidified laterite by-product. *Chem. Eng. J.* **2013**, 228, 565–574. [CrossRef]
- 38. Partey, F.; Norman, D.; Ndur, S.; Nartey, R. Arsenic sorption onto laterite iron concretions: Temperature effect. *J. Colloid Interface Sci.* **2008**, 321, 493–500. [CrossRef]
- 39. Jahan, N.; Guan, H.; Bestland, E.A. Arsenic remediation by Australian laterites. Environ. Earth Sci. 2011, 64, 247–253. [CrossRef]
- 40. Joussein, E.; Petit, S.; Decarreau, A. Une nouvelle méthode de dosage des minéraux argileux en mélange par spectroscopie IR. *Comptes Rendus L'académie Sci.-Ser. IIA-Earth Planet.* **2001**, 332, 83–89. [CrossRef]
- 41. Lakshmipathiraj, P.; Narasimhan, B.R.V.; Prabhakar, S.; Raju, G.B. Adsorption of arsenate on synthetic goethite from aqueous solutions. *J. Hazard. Mater.* **2006**, *136*, 281–287. [CrossRef]
- 42. Madejová, J. FTIR techniques in clay mineral studies. Vib. Spectrosc. 2003, 31, 1–10. [CrossRef]
- 43. ALzaydien, A.S. Adsorption of methylene blue from aqueous solution onto a low-cost natural Jordanian Tripoli. *Am. J. Appl. Sci.* **2009**, *6*, 1047–1058. [CrossRef]
- 44. Kloprogge, J.T.; Frost, R.L.; Hickey, L. Infrared emission spectroscopic study of the dehydroxylation of some hectorites. *Thermochim. Acta* **2000**, 345, 145–156. [CrossRef]
- 45. Ristić, M.; Musić, S.; Godec, M. Properties of γ-FeOOH, α -FeOOH and α -Fe₂O₃ particles precipitated by hydrolysis of Fe³⁺ ions in perchlorate containing aqueous solutions. *J. Alloys Compd.* **2006**, *417*, 292–299. [CrossRef]
- 46. Chen, Y.F.; Wang, M.C.; Hon, M.H. Phase transformation and growth of mullite in kaolin ceramics. *J. Eur. Ceram. Soc.* **2004**, 24, 2389–2397. [CrossRef]
- 47. Sarkar, M.; Banerjee, A.; Pramanick, P.P.; Sarkar, A.R. Design and operation of fixed bed laterite column for the removal of fluoride from water. *Chem. Eng. J.* **2007**, *1*, 329–335. [CrossRef]
- 48. Gallios, G.P.; Tolkou, A.K.; Katsoyiannis, I.A.; Stefusova, K.; Vaclavikova, M.; Deliyanni, E.A. Adsorption of arsenate by nano scaled activated carbon modified by iron and manganese oxides. *Sustainability* **2017**, *9*, 1684. [CrossRef]
- 49. Sanou, Y.; Pare, S.; Nguyen, T.T.; Phuoc, N.V. Experimental and Kinetic modeling of As (V) adsorption on Granular Ferric Hydroxide and Laterite. *J. Environ. Treat. Tech.* **2016**, *4*, 62–70.
- 50. Nguyen, P.T.N.; Abella, L.C.; Gaspillo, P.D.; Hinode, H. Removal of arsenic from simulated groundwater using calcined laterite as the adsorbent. *J. Chem. Eng. Jpn.* **2011**, *44*, 411–419. [CrossRef]
- 51. Uddin, M.K. A review on the adsorption of heavy metals by clay minerals, with special focus on the past decade. *Chem. Eng. J.* **2017**, *308*, 438–462. [CrossRef]
- 52. Cheng, C.H.; Lehmann, J.; Engelhard, M.H. Natural oxidation of black carbon in soils: Changes in molecular form and surface charge along a climosequence. *Geochim. Cosmochim. Acta* **2008**, 72, 1598–1610. [CrossRef]
- 53. Lawrinenko, M.; Laird, D.A. Anion exchange capacity of biochar. Green Chem. 2015, 17, 4628–4636. [CrossRef]
- 54. Schell, W.R.; Jordan, J.V. Anion-exchange studies of pure clays. Plant Soil 1959, 10, 303–318. [CrossRef]
- 55. Achour, S.; Youcef, L. Elimination du Cadmium Par Adsorption Sur Bentonites Sodique et Calcique. Larhyss J. 2003, 2, 68–81.

Minerals **2025**, 15, 379 24 of 24

56. Youcef, L.; Achour, S. Elimination du cuivre par des procédés de précipitation chimique et d'adsorption. *Courr. Savoir* **2006**, 7, 59–65.

- 57. Maji, S.K.; Pal, A.; Pal, T. Arsenic removal from real-life groundwater by adsorption on laterite soil. *J. Hazard. Mater.* **2008**, *151*, 811–820. [CrossRef]
- 58. Sorgho, B.; Paré, S.; Guel, B.; Zerbo, L.; Traoré, K.; Persson, I. Etude d'une argile locale du Burkina Faso à des fins de décontamination en Cu²⁺, Pb²⁺ et Cr³⁺. *J. Société Ouest-Africaine Chim.* **2011**, *31*, 49–59.
- 59. Alshaebi, F.Y.; Yaacob, W.Z.W.; Samsudin, A.R. Removal of arsenic from contaminated water by selected geological natural materials, Aust. *J. Basic Appl. Sci.* **2010**, *4*, 4413–4422.
- 60. Ghorbel-Abid, I.; Galai, K.; Trabelsi-Ayadi, M. Retention of chromium (III) and cadmium (II) from aqueous solution by illitic clay as a low-cost adsorbent. *Desalination* **2010**, 256, 190–195. [CrossRef]
- 61. Tekin, N.; Kadinci, E.; Demirbaş, Ö.; Alkan, M.; Kara, A. Adsorption of polyvinylimidazole onto kaolinite. *J. Colloid Interface Sci.* **2006**, 296, 472–479. [CrossRef]
- 62. Ayari, F.; Srasra, E.; Trabelsi-Ayadi, M. Characterization of bentonitic clays and their use as adsorbent. *Desalination* **2005**, *185*, 391–397. [CrossRef]
- 63. Kouadio, L.M.; Lebouachera, S.I.; Blanc, S.; Sei, J.; Miqueu, C.; Pannier, F.; Martinez, H. Characterization of Clay Materials from Ivory Coast for Their Use as Adsorbents for Wastewater Treatment. *J. Miner. Mater. Charact. Eng.* **2022**, *10*, 319–337. [CrossRef]
- 64. Zhang, X.; Hong, H.; Li, Z.; Guan, J.; Schulz, L. Removal of azobenzene from water by kaolinite. *J. Hazard. Mater.* **2009**, 170, 1064–1069. [CrossRef] [PubMed]
- 65. Mostafapour, F.K.; Bazrafshan, E.; Farzadkia, M.; Amini, S. Arsenic Removal from Aqueous Solutions by Salvadora persica Stem Ash. *J. Chem.* **2013**, 2013, 740847.
- 66. Ayach, J.; Duma, L.; Badran, A.; Hijazi, A.; Martinez, A.; Bechelany, M.; Baydoun, E.; Hamad, H. Enhancing Wastewater Depollution: Sustainable Biosorption Using Chemically Modified Chitosan Derivatives for Efficient Removal of Heavy Metals and Dyes. *Materials* 2024, 17, 2724. [CrossRef] [PubMed]
- 67. Khater, D.; Alkhabbas, M.; Al-Ma'abreh, A.M. Adsorption of Pb, Cu, and Ni Ions on Activated Carbon Prepared from Oak Cupules: Kinetics and Thermodynamics Studies. *Molecules* **2024**, 29, 2489. [CrossRef]
- 68. Chuang, Y.; Chen, J.; Lu, J.; Su, L.; Jiang, S.Y.; Zhao, Y.; Lee, C.H.; Wu, Z.; Ruan, H.D. Sorption studies of Pb(II) onto montmorillonite clay. *IOP Conf. Ser. Earth Environ. Sci.* 2022, 1087, 012007. [CrossRef]
- 69. Pham, T.D.; Pham, T.T.; Phan, M.N.; Ngo, T.M.V.; Dang, V.D.; Vu, C.M. Adsorption characteristics of anionic surfactant onto laterite soil with differently charged surfaces and application for cationic green removal. *J. Mol. Liq.* **2020**, *301*, 112456. [CrossRef]
- 70. Rathore, V.K.; Dohare, D.K.; Mondal, P. Competitive adsorption between arsenic and fluoride from binary mixture on chemically treated laterite. *J. Environ. Chem. Eng.* **2016**, *4*, 2417–2430. [CrossRef]
- 71. Chatterjee, S.; De, S. Application of novel, low-cost, laterite-based adsorbent for removal of lead from water: Equilibrium, kinetic and thermodynamic studies. *J. Environ. Sci. Health—Part A Toxic/Hazard. Subst. Environ. Eng.* **2016**, *51*, 193–203. [CrossRef]
- 72. Bakouan, C. Caractérisation de Quelques Sites Latéritiques du Burkina Faso: Application à L'élimination de L'arsenic (III) et (V) Dans Les Eaux Souterraines. Ph.D. Thesis, Université de Ouaga I Pr Joseph KI-ZERBO, Ouagadougou, Burkina Faso, Université de Mons, Mons, Belgium, 2018; pp. 1–241. Available online: https://orbi.umons.ac.be/bitstream/20.500.12907/31806/1/Th%C3 %A8se (accessed on 1 February 2018).

Disclaimer/Publisher's Note: The statements, opinions and data contained in all publications are solely those of the individual author(s) and contributor(s) and not of MDPI and/or the editor(s). MDPI and/or the editor(s) disclaim responsibility for any injury to people or property resulting from any ideas, methods, instructions or products referred to in the content.